Bacillus thuringiensis Cytolytic Toxin Associates Specifically with Its Synthetic Helices A and C in the Membrane Bound State. Implications for the Assembly of Oligomeric Transmembrane Pores†

Ehud Gazit,‡ Noga Burshtein,‡ David J. Ellar,§ Trevor Sawyer,§ and Yechiel Shai*,‡

Department of Membrane Research and Biophysics, Weizmann Institute of Science, Rehovot 76100, Israel, and Department of Biochemistry, University of Cambridge, Cambridge CB2 1GA, U.K.

Received April 1, 1997; Revised Manuscript Received October 10, 1997⊗

ABSTRACT: The CytA toxin exerts its activity by the formation of pores within target cell membranes. However, the exact mechanism of pore formation and the structural elements that are involved in the toxic activity are yet to be determined. Recently, the structure of the highly similar CytB toxin was solved (Li et al., 1996), and a β-barrel was suggested as a possible structure of the pores. Due to the similarity between the toxins, the existence and positioning of α-helices and β-sheets in CytA were predicted from the alignment of the sequences. Here peptides corresponding to β5, β6, and β7 strands, to a conserved nonhelical region of the CytA toxin ($P^{149-170}$), to helices B and D, and to an analogue of helix A were synthesized, fluorescently labeled, and characterized. We found that, unlike helices A and C (Gazit and Shai, 1993), neither the β-strand peptides nor helix B could interact with lipid membranes, whereas $P^{149-170}$ and helix D bind the membrane weakly. Membrane permeation experiments suggested that CytA toxin exerts its activity by aggregation of several monomers. To learn about the structural elements that may mediate CytA oligomerization, the ability of the synthetic peptides to interact with membrane-bound CytA was studied. Helices A and C, but not the β-strands, helix D, or a control peptide, caused a large increase in the fluorescence of membrane-bound fluorescein-labeled CytA, whereas helix B had only a slight effect. Moreover, the addition of rearranged helix A, a peptide with the same composition as helix A, but with only two pairs of amino acids rearranged, did not affect the fluorescence. The addition of unlabeled CytA also caused an increase in the fluorescence intensity, further demonstrating the interaction between CytA monomers within the membrane. Taken together, our results provide further support for the suggestion that the CytA toxin self-assembles within membrane and that helices A and C are major structural elements involved in the membrane interaction and intermolecular assembly of the toxin.

The Gram-positive bacterium *Bacillus thuringiensis* ssp. *israelensis* (Bti[1]) produces parasporal protein inclusions that are highly toxic to Dipteran insects (*1*). A major component of these inclusions is the 27 kDa protein termed CytA (abbreviation of cytolytic A). The gene encoding the CytA protein was cloned and sequenced (*2*, *3*). A very close homologue (only one amino acid change) was cloned from *B. thuringiensis* ssp. *morrisoni* PG14 (*4*).

Many studies have been conducted on the *in vivo* and *in vitro* activities of CytA. Upon proteolytic activation, CytA is highly cytolytic to a wide range of cells (*5*, *6*). The broad cytolytic activity *in vitro* has been attributed to its hydrophobicity and its ability to bind zwitterionic phospholipids (*5*, *6*). The suggestion that CytA acts by the formation of pores in cell membranes, leading to colloid-osmotic lysis (*7*), is supported by experiments with liposomes and lipid bilayers. CytA induces leakage of low molecular weight substances from lipid vesicles (*8*, *9*) and forms cation-selective single channels in planar bilayers with fast flickering between open and closed states (*10*). Studies on the kinetics of cellular disruption of function of insect Malpighian tubules by CytA suggested that the toxic effect occurs as the result of aggregation of several toxin molecules assumed to form a pore (*11*). Solute exclusion studies have shown that the size of the pore created by CytA is 10−20 Å in diameter (*8*). However, the molecular architecture of the postulated pores formed by the toxin and the structural elements involved in the pore formation process are yet to be determined.

A protein that is highly similar to CytA was cloned and sequenced from *B. thuringiensis* ssp. *kyushuensis* and was designated CytB (*12*). CytA and CytB show 39% identity and 70% similarity in their amino acid sequences (*12*, *13*) (Figure 1B). The three-dimensional structure of CytB was recently determined using X-ray crystallography (*14*). The toxin is composed of two outer layers of α-helix hairpins, wrapped around mixed β-sheets (Figure 1A). Due to the high similarity between CytA and CytB, the existence and positioning of α-helices and β-sheets in CytA were predicted from the alignment of the CytA and CytB sequences (*14*) (Figure 1B).

Peptides corresponding to helices A and C of CytA (*15*) (formerly helices 1 and 2, respectively, in ref 16) and part

† This research was supported in part by the Basic Research Foundation administered by the Israel Academy of Sciences and Humanities. E.G. is a recipient of a doctoral fellowship from the Clore Foundation Scholar Program.

* To whom correspondence should be addressed. Tel: +972-8-9342711. Fax: +972-8-9344112. E-mail: bmshai@weizmann.weizmann.ac.il.

‡ Weizmann Institute of Science.

§ University of Cambridge.

⊗ Abstract published in *Advance ACS Abstracts,* November 15, 1997.

[1] Abbreviations: BOC, butyloxycarbonyl; Bti, *Bacillus thuringiensis* ssp. *israelensis*; CD, circular dichroism; Flu, carboxyfluorescein; LUV, large unilamellar vesicles; PBS, phosphate-buffered saline; PC, egg phosphatidylcholine; SUV, small unilamellar vesicles; TFA, trifluoroacetic acid.

S0006-2960(97)00758-7 CCC: $14.00

A

B

```
CytA 1 M--ENLNHCPLEDIKVNPWKTP--QSTARVITLRVEDPNEINNLLSINEIDNPNYILQAI
       *   *      *    *     *       : * * *    :::*  ::  :: *:** **:
CytB 1 MYTKNFSNSRMEVKGNNGCSAPIIRKPFKHIVLTVPS-SDLDNFNTVFYVQ-PQYINQAL
                        ---------[  β1   ]------[  β2 ]------[ αA

    57 MLANAFQNALVPTSTDFGDALRFSMPKGLEIANTITPMGAVVSYVDQNVTQTNNQVSVMI
        ****** *: *          * *   *:*:*** * *  *:*  ::* * *   ::***:
    59 HLANAFQGAIDPLN------LNFNFEKALQIANGI-PNSAIVKTLNQSVIQQTVEISVMV
          ]------------------[  αb  ]------[      β3      ][  αC

   117 NKVLEVLKTVLGVAL-SGSVIDQLTAAVTNTFTNLNTQKNEAWIFWGKETANQTNYTYNV
       : :  ::  ***: : * *  : : * :  *****:** :******    :* :* * **:
   112 EQLKKIIQEVLGLVINSTSFWNSVEATIKGTFTNLDTQIDEAWIFWHSLSAHNTSYYYNI
             ]-------[   αD    ]--------------[ β4 ]----[  β5

   176 LFAIQNAQTGGVMYCVPVGFEIKVSAVKEQVLFFTIQDSASYNVNIQSLKFAQPLVSSSQ
       **:*** :**:**  :*::**: *   *: ****** *** *:*   :*   * * ** :
   172 LFSIQNEDTGAVMAVLPLAFEVSVDVEKQKVLFFTIKDSARYEVKMKALTLVQALHSS-N
         ]-------[    β6     ]-----[ αE ]---[      β7      ]------

   236 YPIADLTSAINGTL
        ** *:    *  *
   231 APIVDIFNVNNYNLYHSNHKIIQNLNLSN
       --[ αF ]-------
```

FIGURE 1: Crystal structure of CytB toxin. (A) A schematic ribbon diagram of a monomer of CytB determined by X-ray crystallography (modified by J. Li from ref 14). The structure shows a three-layered α/β architecture where the helices form the outer layer and the β-sheets are buried within the core of the protein. Helices A−D are shaded. The α-helices and β-strands are marked according to their designation in ref 14. (B) Alignment of CytA and CytB sequences with the secondary structure elements in CytB.

of helix C (*17*) were synthesized and characterized (*15*, *17*). CD spectroscopy showed that the peptides are helical in methanol and in their membrane-bound state (*15*, *17*). A significant α-helical content in aqueous solution was found for the full-length helix C (*15*) and its 11 amino acid fragment (*17*). This suggested that the secondary structure of the helices is energetically stable regardless of the context of the intact protein, and therefore the helices may serve as autonomous structural elements needed for the activity of the toxin. In addition, a peptide corresponding to amino acids 149−170 ($P^{149-170}$), formerly designated "helix 3" in ref 16, was found to be nonhelical either in hydrophobic solvents or in aqueous solution (*18*), consistent with the fact that this region contains no α-helix in the crystal structure of the highly similar CytB toxin (*14*) (Figure 1A). Biophysical characterization of helices A and C indicated that they were able to bind to phospholipid membranes with high affinity, and to self-assemble and coassemble within membranes (*15*). The studies also indicated that a peptide corresponding to helix C has strong membrane-permeating (*15*) and hemolytic (*17*) activities. Moreover a mutation in helix C of CytA was the only mutation, in a large site-directed mutagenesis study, that increased the hemolytic activity of the toxin (*16*). These results led to the suggestion that CytA helices A and C may have a direct role in the formation of pores by CytA (*15*). However, in light of the crystal structure of the CytB toxin (*14*) (Figure 1A), a different mechanism for pore formation by Cyt toxins was suggested (*14*). According to the model, the pore is built up of a β-barrel structure. The model was suggested because the helices in the X-ray structure are too short to span the 30 Å thickness of the membrane, while the β-sheets are amphipathic or hydrophobic and are long enough to span the lipid membrane to form an aqueous pore. Nevertheless, the length of the helices in the membrane-bound state of the toxin may be significantly different from their length in the toxin crystallized from solution. It was previously demonstrated that membrane-permeating bioactive peptides such as pardaxin, cecropin, and melittin can undergo a significant structural change in their secondary structure upon membrane binding (*19*−*21*).

In this study we investigated the possible involvement of segments derived from CytA in membrane binding and its self-assembly, in light of the recently solved X-ray structure of CytB. We also examined the membrane-permeating activity of the full-length CytA in order to gain insight into its mode of action. The results revealed that peptides corresponding to β5, β6, or β7 strands, alone or in any combination, and a peptide corresponding to helix B do not bind phospholipid membranes, whereas $P^{149-170}$ peptide, which includes the β4 strand, and helix D bind the membrane with lower affinity than helices A and C. Furthermore, helices A and C and to a much lower extent helix B, but not any other peptide studied, could interact with membrane-bound CytA. The results also suggest that CytA permeates membranes by the aggregation of several toxin molecules. Taken together, our results further support a major role for helices A and C of CytA in its binding to phospholipid membranes and in the assembly of toxin monomers to form transmembrane pores.

EXPERIMENTAL PROCEDURES

Materials. BOC amino acids PAM [(phenylacetamido)-methyl] resins were purchased from Applied Biosystems (Foster City, CA), and BOC amino acids were obtained from Bachem Laboratories (Bubendorf, Switzerland). Other reagents for peptide synthesis included trifluoroacetic acid (TFA) (Sigma), *N*,*N*-diisopropylethylamine (DIEA) (Aldrich, distilled over ninhydrin), dicyclohexylcarbodiimide (DCC) (Fluka), 1-hydroxybenzotriazole (HOBT) (Pierce), and methylene chloride and dimethylformamide (DMF) (Bio-lab). Egg phosphatidylcholine (PC) was purchased from Lipid Products (South Nutfield, U.K.). Cholesterol (extra pure) and Proteinase-K were supplied by Merck (Darmstadt, Germany). The cholesterol was recrystallized twice from ethanol. Immobilized proteinase-K was supplied by Sigma. Carboxyfluorescein was obtained from Molecular Probes (Eugene, OR). All other reagents were of analytical grade. Buffers were prepared in double-glass-distilled water.

Isolation and HPLC Gel Filtration of Protein Inclusions. The CytA gene from *B. thuringiensis* ssp. *israelensis* was expressed in an acrystalliferous *B. thuringiensis* strain (IPS78/11) in which it is produced as inclusion bodies (*22*). The methods used for growth of this strain and purification of inclusions have been described previously (*23*). CytA was solubilized by incubation with 50 mM sodium carbonate pH 10.5 at 37 °C for 2 h. The supernatant was then dialyzed

against double-distilled H_2O and lyophilized. The lyophilized toxin was solubilized again by incubation with 50 mM sodium carbonate pH 10.5 at 37 °C for 30 min and subjected to HPLC gel filtration using a Bio-Sil TSK-125 column (600 × 7.5 mm, Bio-Rad). The running buffer was PBS at a flow rate of 1 mL/min. In order to determine the aggregation state of the soluble CytA in solution, gel filtration HPLC was used. The preparations of soluble CytA used in this study were found to be predominantly (over 90%) monomeric. A small peak (less than 5%) of the dimeric form was also observed (data not shown).

Fluorescent Labeling of CytA. A suspension of CytA was reacted with carboxyfluorescein succinimidyl ester (Flu-suc) (20 equiv) in PBS. After 24 h of incubation, the mixture was washed thoroughly with the same buffer and was dialyzed against double-distilled water to remove the excess of nonbound fluorescent probe, followed by lyophilization. The lyophilized toxin was then solubilized again in 50 mM sodium carbonate pH 10.5, at 37 °C for 30 min (*5*, *6*). The concentration of CytA was determined by amino acid analysis. The ratio between the fluorescence intensity of denaturated toxin and the concentration of the protein indicated 0.38 ± 0.02 fluorescent probes per protein molecule. In order to determine the site of the labeling, labeled CytA toxin was proteolytically digested and the fluorescence of the resulted peptide fragment was determined. Labeled toxin (50 μg) was solubilized in a 200 mM ammonium bicarbonate and reacted with trypsin (1 μg) for 2 h at 37 °C. The reaction mixture containing the peptide fragments was then lyophilized and redissolved in 10% acetonitrile in water containing 0.1% TFA (v/v). The peptide fragments were purified on a reversed phase Bio-Rad analytical column (250 × 10 mm, 300 Å pore size, 5 μm particle size) using a DAD (diode array detector)-equipped HPLC. The column was eluted in 40 min, using a linear gradient of 0−80% acetonitrile in water containing 0.05% TFA (v/v), at a flow rate of 0.6 mL/min. The HPLC profile of the digested labeled protein revealed the existence of two fluorescein-labeled peptide fragments. Proteinase-K activation of the toxin removed a labeled fragment. Since this activation cuts 30 amino acids from the N-terminal domain of CytA, activated CytA is probably labeled on one lysine located in a solvent-exposed loop.

Peptide Synthesis. The synthesis of helices A and C (*15*) and cecropin B2 (*21*) was described previously. Peptides corresponding to β5, β6, β7, $P^{149-170}$, helix B, helix D, and rearranged helix A were synthesized by a solid-phase method on PAM resins using *t*-Boc chemistry. The resin-bound peptides were cleaved from the resins by hydrogen fluoride (HF) and finally extracted with dry ether after HF evaporation. The synthesized peptides were purified by RP-HPLC on a C_{18} reverse phase Vydac semipreparative column. The column was eluted in 40 min, using a linear gradient of 10−80% acetonitrile for β5, β6, and β7, 0−80% acetonitrile for $P^{149-170}$ and helix B, or 25−80% acetonitrile for rearranged helix A and helix D, all in water containing 0.1% TFA (v/v), at a flow rate of 1.8 mL/min. The purified peptides were shown to be homogeneous (∼99%) by analytical HPLC. The peptides were subjected to amino acid analysis to confirm their compositions.

Fluorescent Labeling of Peptides. Labeling of the N-terminus of the peptides with the NBD fluorescent probe was achieved by labeling the resin-bound peptides as previously described (*24*). Briefly, 10 mg samples of resin-bound peptides (3−4 μmol) were treated with TFA (50% v/v in methylene chloride) in order to remove the BOC protecting group from the N-terminal amino groups of the linked peptides. The resin-bound peptides were then reacted with NBD-F in dry dimethylformamide. The peptides were cleaved from the resins by HF and finally precipitated with ether. All peptides were purified using RP-HPLC as described in the previous section.

CD Spectroscopy. The CD spectra of the peptides were measured with a Jasco J-500A spectropolarimeter. The spectra were scanned at room temperature in a capped, quartz optical cell with a 0.5 mm pathlength. Spectra were obtained at wavelengths of 250 to 195 nm. Eight scans were taken at a scan rate of 20 nm/min for each peptide. The peptides were scanned at concentrations of 2.0×10^{-5} M in methanol and in buffer (50 mM Na_2SO_4, 25 mM HEPES-sulfate, pH 6.8). Fractional helicities were calculated as follows

$$f_h = \frac{([\theta]_{222} - [\theta]^0_{222})}{[\theta]^{100}_{222}} \quad (1)$$

where $[\theta]_{222}$ is the experimentally-observed mean residue ellipticity at 222 nm, and the values for $[\theta]^0_{222}$ and $[\theta]^{100}_{222}$, which correspond to 0% and 100% helix content at 222 nm, are estimated at −2000 and −30 000 deg·cm^2/dmol, respectively.

Preparation of Large and Small Unilamellar Vesicles (LUV and SUV). LUV were prepared from phospholipids as follows. Dry PC phospholipids and cholesterol were dissolved in $CHCl_3$/MeOH (2:1 v/v) such that the mixture contained 10% (w/w) cholesterol. The solvents were evaporated under a stream of nitrogen. The lipid film was hydrated in buffer and dispersed by vortexing to produce large multilamellar vesicles. The lipid suspension was freeze−thawed five times and then extruded through polycarbonate membrane filters (Poretics Corporation, Livermore, CA) in an extruder (Lipex Biomembranes Inc., Vancouver, B.C., Canada) twice with a pore diameter of 0.4 μm and then eight times with a pore diameter of 0.1 μm (*25*). The size distribution of the vesicles was determined by dynamic light scattering in a Malvern 4700 submicron particle analyzer. The mean diameter was found to be 113 nm.

SUV were prepared by sonication of hydrated PC that contained 10% (w/w) cholesterol mixture as described in detail elsewhere (*15*). Vesicles were visualized by using a JEOL JEM 100B electron microscope (Japan Electron Optics Laboratory Co. Tokyo, Japan) as follows: A drop of vesicles was deposited on a carbon-coated grid and negatively stained with uranyl acetate (2%, pH 4.8). The grids were examined, and the vesicles were shown to be unilamellar with an average diameter of 30−50 nm.

Binding Experiments. Binding experiments were conducted as previously described (*15*, *24*). Briefly, SUV were added successively to 0.1 μM NBD-labeled peptides at room temperature. Fluorescence intensity was measured as a function of the lipid:peptide molar ratio on a Perkin-Elmer LS-50B spectrofluorimeter, with excitation set at 467 nm, using a 10 nm slit, and emission was monitored at 530 nm, using a 5 nm slit, in three separate experiments. In order to account for the background signal contributed by the lipids

Table 1: Amino Acid Sequences of the Peptides Used in the Study

designation	sequence
helix A	NH_2-N Y I L Q A I M L A N A F Q N A L V P T S T-COOH
rearranged helix A[a,b]	X-NH-N Y I Q M A I Q L A N A F L N A L V P T S T-COOH
helix B	X-NH-D F G D A L R F S M P K G L E I A N T I T-COCH
helix C	NH_2-N Q V S V M I N K V L E V L K T V L G V A L-COOH
helix D	X-NH-G S V I D Q L T A A V T N T F T L N-COOH
$P^{149-170}$ [b]	X-NH-N L N T Q K N E A W I F W G K E T A N Q T N-COOH
β5 strand[b]	X-NH-N Q T N Y T Y N V L F A I-COOH
β6 strand[b]	X-NH-G V M Y C V P V G F E I K V-COOH
β7 strand[b]	X-NH-S A S Y N V N I Q S L K F A Q-COOH
cecropin B2[c]	NH_2-R W K I F K K I E K M G R N I R D G I V K A G P A I E V L G S A K A I-NH_2

[a] Rearranged amino acids are underlined. [b] X = H, NBD. [c] Taken from Gazit et al. (1994).

to any given signal, the readings of lipid vesicles alone were subtracted from the recordings of fluorescence intensity.

The binding isotherms were analyzed as partition equilibria (*26*−*28*) as described in detail in several other studies (*15*, *21*, *24*), using the following formula

$$X_b^* = K_p^* C_f \quad (2)$$

were X_b^* is defined as the molar ratio of bound peptide per 60% of the total lipid as had been previously suggested (*28*), K_p^* corresponds to the partition coefficient, and C_f represents the equilibrium concentration of free peptide in solution.

The curve that results from plotting X_b^* versus free peptide, C_f, is referred to as the conventional binding isotherm.

Hemolytic Activity. Activated labeled and nonlabeled toxin molecules were incubated for 2 h at 37 °C with prewashed 0.1% v/v human erythrocytes dissolved in PBS. Nonlysed erythrocytes were sedimented by centrifugation, and hemolytic activity was determined by reading the absorbance of the released hemoglobin at 405 nm using a 96-well plate on a BIO-TEK instruments auto plate reader.

Membrane Permeation Induced by the Toxin. Membrane permeation was assessed utilizing the diffusion potential assay (*29*) as previously described (*19*). In a typical experiment, 4 μL (28.8 μg) of a liposome suspension, prepared in a K^+-containing buffer (50 mM K_2SO_4, 25 mM HEPES-SO_4^{2-}, pH 6.8), was diluted in 1 mL of an isotonic K^+-free buffer (50 mM Na_2SO_4, 25 mM HEPES-SO_4^{2-}, pH 6.8) in a glass tube to which the fluorescent, potential-sensitive dye diS-C_2-5 was then added. Valinomycin (1 μL of 10^{-7} M) was added to the suspension in order to slowly create a negative diffusion potential inside the vesicles, which led to a quenching of the dye's fluorescence. Once the fluorescence had stabilized, 10−15 min later, CytA was added. The subsequent dissipation of the diffusion potential, as reflected by an increase in fluorescence, was monitored on a Perkin-Elmer LS-50B spectrofluorimeter, with excitation set at 620 nm and emission at 670 nm, and the gain adjusted to 100%. The percentage of fluorescence recovery, F_t, was defined as

$$F_t = [(I_t - I_0)/(I_f - I_0)] \times 100 \quad (3)$$

where I_0 = the initial fluorescence, I_f = the total fluorescence observed before the addition of valinomycin, and I_t = the fluorescence observed after adding the peptide, at time *t*.

Interaction of the Peptides with Membrane-Bound Flu-CytA. Synthetic peptides or unlabeled CytA protein were added to a solution containing Flu-CytA preincubated with 20 μL of PC LUV (2 mg/mL) membranes in PBS. The degree of change in protein fluorescence was determined by measuring the increase in the intensity of fluorescence, using a Perkin-Elmer LS-50B spectrofluorimeter with the excitation monochromator set at 480 nm and emission set at 520 nm. Measurements were performed in a 1 cm pathlength glass cuvette and a final reaction volume of 2 mL. The change in fluorescence intensity is presented as the fraction of fluorescence after peptide addition (F) divided by the initial fluorescence (F_0).

RESULTS

To gain insight into the structural elements that may be involved in the pore formation activity of CytA, the ability of various synthetic peptides corresponding to different parts of the toxin to interact with phospholipid membrane and with membrane-bound CytA was studied. The list includes peptides corresponding to helices A, B, C, and D, to β-strands β5, β6, β7, to a rearranged helix A (Re-helix A, in which the positions of two pairs of amino acids were exchanged; L4 with Q14, and Q5 with M8), to a highly conserved nonhelical region (amino acids 149−170) which contains β4, and to the antibacterial peptide cecropin to serve as a control. The peptides and their designations are listed in Table 1. To gain further insight into the mode of action of CytA, its ability to permeate SUV and LUV was also studied.

Hemolytic Activity of Labeled CytA. The effect of the fluorescence labeling on the biological activity of the protein was examined by comparing the ability of the intact CytA and its fluorescently labeled analogue to lyse human erythrocytes. The hemolytic activity of the activated labeled toxin was not significantly different from that of the unlabeled activated toxin (Figure 2). The activity of the labeled toxin is consistent with site-directed mutagenesis studies (*16*) that demonstrated that, upon mutating several basic residues into neutral amino acids, the hemolytic activity of the toxin is either not affected considerably (Lys^{83}, Lys^{118}, Lys^{195}) or even increased (Lys^{124}). Since the broad CytA cytolytic activity is probably not mediated via binding to a receptor (*5*, *6*, *14*), it is reasonable to assume that the basic amino acids that were accessible to the fluorescence labeling are solvent-exposed residues on the surface of the toxin molecule and thus may not have a role in the pore-forming abilities of the protein. Tryptic digestion of the peptide revealed two major fluorescent fragments. One site may be the N-terminal amino group of the toxin which is the most active site under the labeling conditions. The other label is probably located at one of the exposed loops. Since

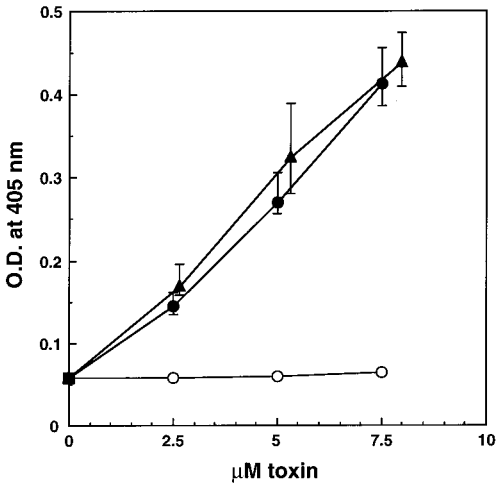

FIGURE 2: Hemolytic activity of CytA toxin and its fluorescently labeled derivative. Degree of hemolysis was determined by reading the absorbance at 405 nm after a 2 h incubation at 37 °C and removal of unlysed cells by centrifugation. Designations: triangles, Flu-CytA; filled circles, CytA; empty circles, 0.1% proteinase-K (control).

activation by proteinase-K cuts 30 amino acids from the N-terminal of CytA, the toxin is left labeled predominantly on one site. The effect of proteinase-K (used for activation of the toxin) on hemoglobin release from the erythrocytes was also studied to rule out any contribution of its activity to the hemolytic activity of the toxin, and it was found to be negligible (Figure 2).

CD Spectroscopy. The secondary structure of the peptides was estimated from their CD spectra in methanol (Figure 3). Re-helix A had a mean residual ellipticity $[\Theta]_{222}$ of −18 630 deg·cm^2/dmol, corresponding to 55.6% α-helical structure. This value is similar to that found for helix A (*15*), suggesting that the rearrangement did not affect significantly the secondary structure of the peptide. The mean residual ellipticities found for helices B and D were −7560 and −7320 deg·cm^2/dmol, respectively, corresponding to 18.5% and 17.7% α-helical structure. This is consistent with the relatively short length (7−12 amino acid) of these helices as found in the X-ray structure of CytB (*14*).

The β-strand peptides β5, β6, β7, and P$^{149-170}$ (which includes β4) had a typical β-structure in methanol (Figure 3B). All the spectra had a single minimum between 210−220 nm with ellipticities not higher than 2000 deg·cm^2/dmol. It should be noted that methanol is known to stabilize secondary structure elements of peptides and proteins.

Characterization of Binding Isotherms and Determination of Partition Constants. The high sensitivity of the NBD probe to the hydrophobicity of its environment enabled us to use it for membrane binding experiments. Upon relocalization of the NBD probe to an environment of increased hydrophobicity a large increase and a blue shift in the fluorescence are observed. An increase of fluorescence and a blue shift in the emission maximum were observed previously for peptides that bind on the surface of membranes (*21*, *30*), as well as for those which insert into the hydrophobic core of membranes (*31*). To study the affinity of the peptides for the membrane, solutions containing NBD-β5, NBD-β6, NBD-β7, NBD-P$^{149-170}$, NBD-helix B, NBD-helix D, or NBD-Re-helix A at a fixed concentration (0.1 μM) were titrated with PC vesicles. When the vesicles were added to a solution containing NBD-β5, NBD-β6, NBD-

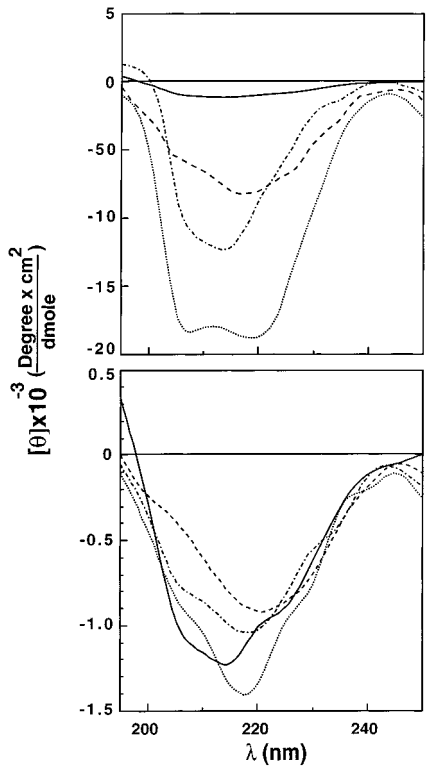

FIGURE 3: CD spectra of the peptides in methanol. Spectra were taken as described by the Experimental Procedures. Panel A: dotted line, Re-helix A; dashed-dotted line, helix D; dashed line, helix B; solid line, β7. Panel BSPCLN dotted line, β5; dashed line, β6; solid line, β7; dashed-dotted line, P$^{149-170}$.

β7, or NBD-helix B, neither an increase nor a shift in the fluorescence of the NBD probe was observed (e.g. NBD-β5 in Figure 4A), even when the [peptide]/[lipid] ratios were elevated to 1:4000. To study whether the inability of the β-strand peptides to bind phospholipid membranes was due to the need of the peptides to form intermolecular complexes with the other strands, the following mixtures of peptides were titrated with the vesicles: (i) NBD-β5 + unlabeled β6 + unlabeled β7; (ii) unlabeled β5 + NBD-β6 + unlabeled β7; (iii) unlabeled β5 + unlabeled β6 + NBD-β7, all in concentrations of 0.1 μM. In all of these experiments no net change in the fluorescence was observed. Furthermore, we tried to incorporate the peptides into the membrane by mixing a solution of NBD-labeled peptides (dissolved in methanol, alone or in a combination with unlabeled peptides) with lipids dissolved in chloroform:methanol, followed by evaporation of the solvents, hydration of the film obtained, and sonication. No increase in the fluorescence was observed in these experiments also. The results suggest that β5, β6, and β7 probably do not have a role in the initial binding of CytA toxin to the lipid membranes.

In contrast, when NBD-P$^{149-170}$, NBD-helix D, or NBD-Re-helix A was titrated with lipid vesicles, increases in the fluorescence were observed (e.g. Figure 4B,C). Plotting of the resulting increases in fluorescence intensities of NBD-labeled peptides as a function of lipid/peptide molar ratios yielded conventional binding curves (Figures 5A, 6A, and 7A for NBD-P$^{149-170}$, NBD-Re-helix A, and NBD-helix D respectively). Since the concentrations of the NBD-labeled peptides in the mixtures were low, the peptides were assumed not to disrupt the bilayer structure. When unlabeled peptides were titrated with lipids, up to the maximal concentration

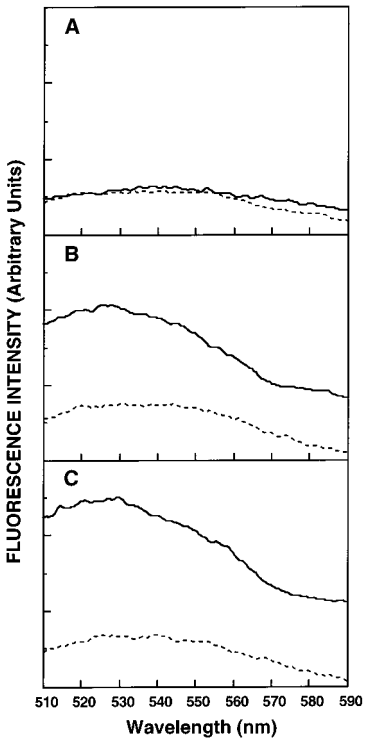

FIGURE 4: Fluorescence emission spectra of NBD-labeled peptides. Spectra of NBD-labeled peptides (0.1 μM) in buffer (50 mM Na_2SO_4, 25 mM HEPES-SO_4^{-2}, pH 6.8) (dashed line) or in the presence of PC SUVs (400 μM) (solid line). The excitation wavelength was 467 nm, and emission was scanned from 510 to 590 nm. Panel A: NBD-β5 (similar results were obtained with NBD-β6 and NBD-β7). Panel B: NBD-$P^{149-170}$. Panel C: NBD-Re-helix A.

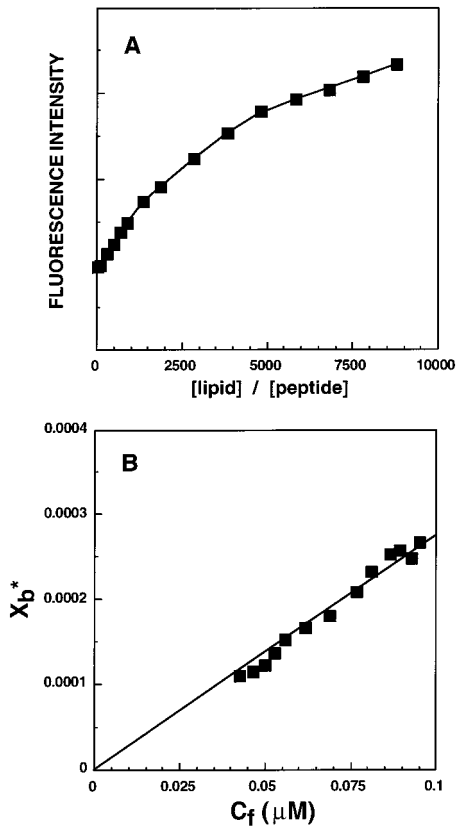

FIGURE 5: Increase in the fluorescence of NBD-$P^{149-170}$ upon titration with PC vesicles (A), and the resulting binding isotherm (B). A: NBD-$P^{149-170}$ (0.1 μM) in 50 mM Na_2SO_4, 25 mM HEPES-SO_4^{-2} was titrated with PC vesicles at 24 °C, the excitation wavelength was 467 nm, and emission was monitored at 530 nm. B: Binding isotherm derived from Figure 5A by plotting X_b* (molar ratio of bound peptide per 60% of lipid) versus C_f (equilibrium concentration of free peptide in the solution).

used with NBD-labeled peptides, the fluorescence intensities of the solutions, after subtracting the contribution of the vesicles, remained unchanged. The curves obtained by plotting X_b* (the molar ratio of bound peptide per 60% of the total lipid) versus C_f (the equilibrium concentration of free peptide in the solution) are referred to as the conventional binding isotherms. The experimental binding isotherms of NBD-$P^{149-170}$ (Figure 5B), NBD-Re-helix A (Figure 6B), and NBD-helix D (Figure 7B) with PC vesicles were determined. The surface partition coefficients were estimated by extrapolating the initial slopes of the curves to C_f values of zero. The estimated surface partition coefficients, K_p*, were $(2.7 \pm 0.6) \times 10^3$ M^{-1}, $(2.1 \pm 0.7) \times 10^3$ M^{-1} and $(2.9 \pm 0.5) \times 10^4$ M^{-1} for NBD-$P^{149-170}$, NBD-helix D, and NBD-Re-helix A, respectively (three measurements each). The K_p* value of $P^{149-170}$ and NBD-helix D are 1 order of magnitude lower than those of helices A and C (*15*). These K_p* values are also lower than those observed with various membrane-permeating bioactive peptides, such as melittin and its derivatives (*32*), the antibiotic dermaseptin (*33*), and pardaxin analogues (*24*). The K_p* value of NBD-Re-helix A and the shape of its binding isotherm are very similar to those of NBD-helix A, suggesting that the rearrangement did not change significantly the membrane binding properties of the peptide.

Specific Interaction between CytA and Its Synthetic Helices within Membranes. In order to depict the structural elements that may be involved in the oligomerization process of CytA within the membrane, the ability of several peptides to interact with membrane-bound activated CytA was studied. Peptides corresponding to helices A and C, rearranged helix A, β5, β6, β7, $P^{149-170}$, and cecropin B2 (an unrelated control peptide) were used.

Upon addition of either helix A or C to a solution containing membrane-bound Flu-CytA, a large increase in its fluorescence emission intensity was observed (Figure 8). However when β5, β6, β7, or $P^{149-170}$ were added, even at a concentration 60-fold higher than the concentration at which helices A and C show activity, no change in the fluorescence emission was detected.

Addition of helix B which does not bind membranes also caused an increase in the fluorescence, albeit significantly less compared to helices A and C (Figure 8), indicating that membrane binding is neither essential nor sufficient for the interaction between the peptides and membrane-bound CytA. Interestingly, Re-helix A, in which the positions of only two pairs of amino acids were exchanged, did not have any effect on the fluorescence of activated Flu-CytA toxin. Since the membrane-binding properties of helix A and rearranged helix A are very similar (as was shown by the binding experiments), the drastic effect of the rearrangement on the activity of the peptide suggests that a specific pattern of amino acid side chains is essential for the assembly process. The rearranged helix A was designed to improve the amphipathicity of helix A. Therefore, the results further prove that the driving force for the interaction is a specific sequence and is not due the amphipathic nature of helix A. The increase in the fluorescence of Flu-CytA may either result from conformational changes within the protein or be due

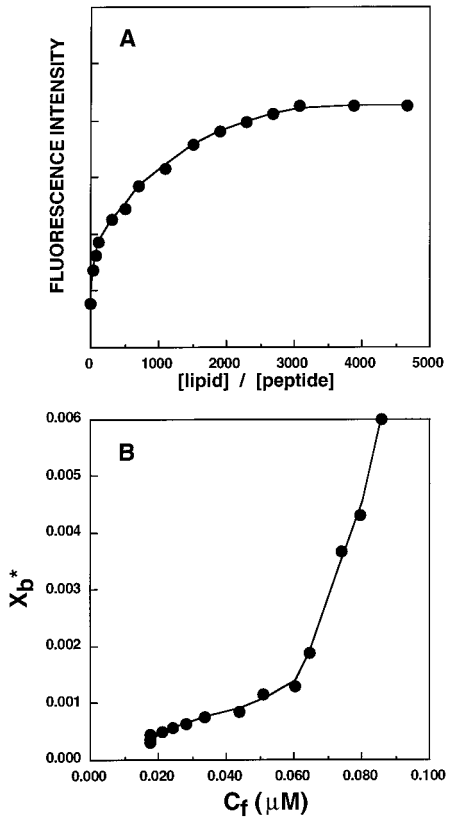

FIGURE 6: Increase in the fluorescence of NBD-Re-helix A upon titration with PC vesicles (A), and the resulting binding isotherm (B). A: The NBD-Re-helix A (0.1 μM) in 50 mM Na_2SO_4, 25 mM HEPES-SO_4^{2-} was titrated with PC vesicles at 24 °C, the excitation wavelength was 467 nm, and emission was monitored at 530 nm. B: Binding isotherm derived from Figure 6A (see legend of Figure 5B).

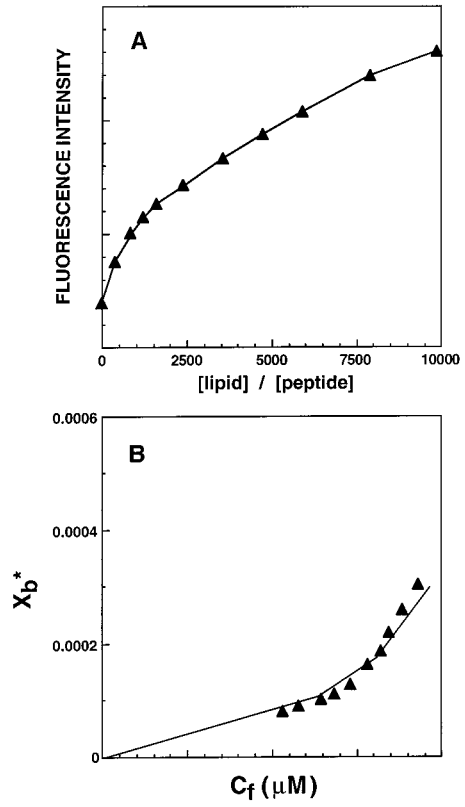

FIGURE 7: Increase in the fluorescence of NBD-helix D upon titration with PC vesicles (A), and the resulting binding isotherm (B). A: NBD-helix D (0.1 μM) in 50 mM Na_2SO_4, 25 mM HEPES-SO_4^{2-} was titrated with PC vesicles at 24 °C, the excitation wavelength was 467 nm, and emission was monitored at 530 nm. B: Binding isotherm derived from Figure 7A (see legend of Figure 5B).

to dissociation of a CytA intermolecular complex. However both effects reveal interaction between the peptides and CytA. The addition of an unrelated peptide, cecropin B2, a surface-localized amphipathic α-helix (*21*), did not affect significantly the fluorescence of CytA.

When unlabeled activated CytA was added to a solution containing membrane-bound Flu-CytA, an increase in the fluorescence intensity was also observed, although to a lesser extent than the effect induced by peptides A and C. This result further demonstrates an interaction between CytA monomers within the membrane environment. It is possible that the pore formed by cytA is more susceptible to the effect of the small peptides as compared to the large protein due to stearic hindrance.

Membrane Permeability Induced by the Toxin. CytA was examined for its efficacy in perturbing the lipid packing and causing leakage of vesicular contents from either SUV or LUV, by utilizing the dissipation of diffusion potential assay. This assay is highly sensitive since it determines the leakage of ions through the membrane. This is in contrast to assays that study the release of entrapped fluorescent material, for which there is a need for a large perturbation of the membrane rather than a small organized pore. Increasing concentrations of CytA were mixed either with PC SUV or PC LUV that had been pretreated with the fluorescent, potential-sensitive dye (diS-C_2-5) and valinomycin. Recovery of fluorescence was monitored as a function of time and usually occurred within 60 min. Maximal activity of CytA was plotted versus CytA/lipid molar ratios (Figure 9). Each

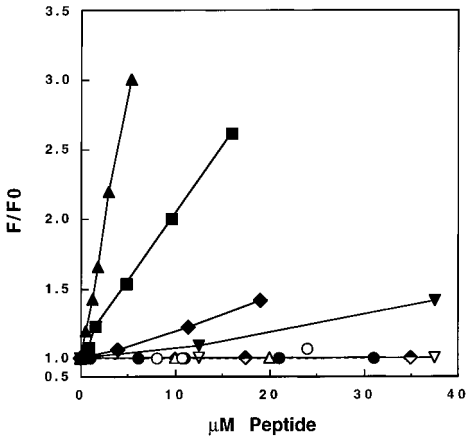

FIGURE 8: Dose−response effect of addition of peptides on the fluorescence of membrane-bound Flu-CytA. Peptides or unlabeled CytA were added to Flu-CytA (final concentration 0.024 μM) preincubated with PC LUV vesicles. The fluorescence intensity after peptide addition (F_x) was divided by the initial fluorescence (F_0). Designation: filled squares, helix A; inverted filled triangles, helix B; filled triangles, helix C; inverted filled triangles, helix D; empty triangles, rearranged-helix A; filled circles, $P^{149-170}$; empty circles, cecropin B2; empty rhomboids, β5 (same results obtained with β6 and β7); filled rhomboids, unlabeled CytA.

point represents the mean of two or three separate experiments with standard deviations of ∼5%. The membrane permeating activity of CytA was significantly higher with PC LUV compared to PC SUV (Figure 9). For example, at the lipid/protein molar ratio of 0.0106, 86.5% and 21.8% of permeating activity is observed for LUV and SUV, respec-

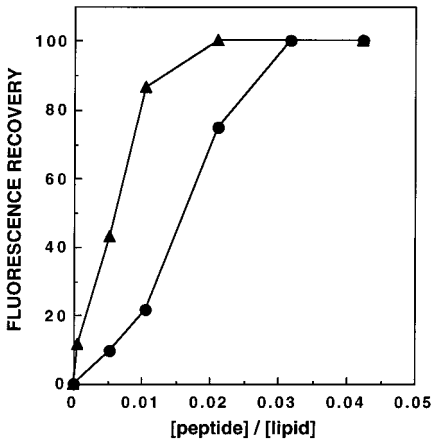

FIGURE 9: Maximal dissipation of the diffusion potential in vesicles induced by the CytA. CytA was added to isotonic K^+−free buffer containing LUV or SUV, pre-equilibrated with the fluorescent dye diS-C_2-5 and valinomycin. Fluorescence recovery, measured 30−40 min after mixing the protein with the vesicles, is shown. Designations are as follows: triangles, LUV; circles, SUV.

tively. These results suggest that the mechanism of membrane permeation is by the formation of distinct transmembrane pores rather than by a detergent-like effect. In the latter case, similar or lower peptide:lipid ratios would be expected for the permeation of SUV as compared to LUV. This is because the permeating activity of a detergent should be proportional to the total surface area of the vesicles which is similar for both SUV and LUV in a same lipid concentration. However if pores are formed and a single pore is sufficient to cause permeation of a single vesicle, a higher activity is expected with LUV due to their lower number compared to SUV, at similar lipid concentrations.

DISCUSSION

Despite the great importance of *B. thuringiensis* δ-endotoxins as the major environmentally safe alternative to chemical pesticides, their precise mechanism of membrane permeation is still to be determined. The Cyt δ-endotoxins are of special interest since their cytolytic activity is assumed to result from lipid−protein interaction rather than to be mediated by receptor binding (*14*). Thus, insights into their mode of action can serve as a paradigm for the much larger group of other membrane-permeating protein toxins that may use similar principles to deliver their toxic activity. The CytA toxin was assumed to act by the formation of transmembrane pores that are built up by the aggregation of several transmembrane amphipathic α-helices, as is probably the correct mode of action of the Cry δ-endotoxin (*34*, *35*). According to this model, the pore is formed by a bundle of transmembrane amphipathic α-helices in which outwardly directed hydrophobic surfaces interact with either the hydrophobic surface of the other helices or the hydrophobic core of the membrane, while inwardly facing hydrophilic surfaces produce the pore. This notion was further supported by the finding that helices A and C have high affinity for phospholipid membranes, coassemble therein, and can induce membrane leakage (*15*).

The X-ray structure of CytB confirmed the α-helical structure of the predicted helices. However, an extensive β-sheet structure was also observed. On the basis of the structure of the transmembrane pore formed by the bacterial porin molecules, it was suggested that the CytB pore may be built up of a β-barrel structure (*14*). To get further insight on the mode of action of CytA, and to determine the structural elements that are involved in its binding and assembly within membranes, peptides corresponding to β5, β6, and β7 β-strands, to a highly conserved nonhelical region of the toxin ($P^{149-170}$), to helices B and D, and to a rearranged analogue of helix A were synthesized. The peptides were then analyzed for their structure and affinity to phospholipid membranes, and together with helices A and C, for their ability to interact with membrane bound CytA.

Our results demonstrate that helix B, β5, β6, or β7 do not have the molecular properties to initiate the binding of CytA to the membrane. The affinities of the highly conserved $P^{149-170}$ and helix D peptides for the membrane are also lower than those of helices A and C and other membrane binding peptides. Taking together these and our previous results, helices A and C seem to be the best candidates that have a significant role in the initial binding of the toxin to the membrane.

CytA is more potent in permeating LUV as compared to SUV as was found in the dissipation of diffusion potential experiments (Figure 9), suggesting that the toxin forms pores in the membrane rather than acting as a detergent. These results are also consistent with studies conducted on the kinetics of cellular disruption function of insect Malpighian tubules by CytA, which suggested that the toxic effect occurs due to aggregation of several toxin molecules that are assumed to form a pore (*11*). Another experimental result in favor of a pore formation mechanism is the formation of selective ion channels in planar lipid bilayers by CytA (*10*). The formation of pores by membrane-permeating toxins generally occurs via a barrel−stave mechanism (for review, see refs 20 and 36). This mechanism involves the sequential addition of monomers to form a pore of a dynamically increasing size. The question that arises is what are the structural elements that are involved in this assumed process of aggregation. To answer this question we studied the ability of the synthetic peptides to interact with fluorescently labeled membrane-bound CytA. The finding that helices A and C interact specifically with CytA (Figure 8) suggests that they both serve as structural elements in the oligomerization process. The results are consistent with our previous studies (*15*), demonstrating that both peptides have the ability to self-assemble and coassemble within phospholipid membranes. On the other hand helix D, β5, β6, β7, or $P^{149-170}$ do not have the structural information needed to mediate such interactions. Helix B may also assist in recognition between CytA monomers, but its role may be secondary to that of helices A and C. An interesting result was the inability of the rearranged helix A to affect the fluorescence of Flu-CytA (Figure 8), despite the fact that the positions of only two pairs of amino acids were exchanged and that both its α-helical structure and affinity to membranes are similar to those of helix A (Figures 3A and 6). This result demonstrates that a specific pattern of amino acid side chains is essential for the peptide−protein recognition process.

The specific interaction between CytA and its helices may explain its high cytolytic activity. The target cell membrane contains a large amount of membrane proteins with different degrees of hydrophobicity and membrane orientation. In order to self-assemble efficiently, CytA must distinguish between its hydrophobic helices and those of other proteins within and near the membrane environment. The oligomer-

ization of many large transmembrane proteins is a crucial step in the establishment of their activity. The location of helices A and C in the outer layer of the toxin (Figure 1A) making them accessible for intermolecular interactions, together with their conservation between CytA and CytB, suggests that a significant part of the intermolecular recognition process leading to the formation of the toxin pore may be mediated by interactions between these helices. The findings that the fluorescence of Flu-CytA is slightly affected by helix B that does not bind the membrane, but is not affected by helix D and Re-helix A, both of which bind the membrane, indicate that membrane binding is neither essential nor sufficient for the interaction between the peptides and membrane-bound CytA. Extramembranous regions in the N-terminal domain of the Shaker K^+ channel have been also shown to control the assembly of the channel (*37*).

CytA oligomerization can also serve as a good model to study specific interactions of membrane-embedded protein segments, since (1) it inserts spontaneously into the membrane and (2) it is compact and has only few helices, which are the principal secondary structural elements for recognition on or within the membrane (*38*). The results reported here also support the accumulating data that α-helices of integral membrane proteins can participate in specific interactions that contribute to a specific recognition, association, and oligomerization of those proteins within the lipid environment (*20*, *39*).

In summary, our results indicate that helices A and C of CytA are the major regions that may contain the structural information for initiating membrane binding and mediating the recognition between CytA molecules to form a pore. Furthermore the data suggest that activated CytA permeates membranes by the formation of aggregates within a phospholipid membrane. Nevertheless, a mechanism of pore formation in which recognition, assembly, and perhaps orientation of toxin monomers within the membrane are driven by helix−membrane interactions while the interior of the pore contains β-strands cannot be ruled out.

REFERENCES

1. Goldberg, L. J., and Margalit, J. (1977) *Mosquito News 37*, 355−358.
2. Ward, E. S., Ellar, D. J., and Todd, J. A. (1984) *FEBS Lett. 175*, 377−382.
3. Waalwijk, C., Dullemans, A. M., van, W. M., and Visser, B. (1985) *Nucleic Acids Res. 13*, 8207−8217.
4. Earp, D. J., and Ellar, D. J. (1987) *Nucleic Acids Res. 15*, 3619.
5. Thomas, W. E., and Ellar, D. J. (1983) *J. Cell Sci. 60*, 181−197.
6. Thomas, W. E., and Ellar, D. J. (1983) *FEBS Lett. 154*, 362−368.
7. Knowles, B. H., and Ellar, D. J. (1987) *Biochim. Biophys. Acta 924*, 509−518.
8. Drobniewski, F. A., and Ellar, D. J. (1988) *Curr. Microbiol. 16*, 195−199.
9. Drobniewski, F. A., and Ellar, D. J. (1989) *J. Bacteriol. 171*, 3060−3067.
10. Knowles, B. H., Blatt, M. R., Tester, M., Horsnell, J. M., Carroll, J., Menestrina, G., and Ellar, D. J. (1989) *FEBS Lett. 244*, 259−262.
11. Maddrell, S. H., Overton, J. A., Ellar, D. J., and Knowles, B. H. (1989) *J. Cell Sci. 94*, 601−608.
12. Koni, P. A., and Ellar, D. J. (1993) *J. Mol. Biol. 229*, 319−327.
13. Knowles, B. H. (1994) *Adv. Insect Physiol. 24*, 275−308.
14. Li, J. D., Koni, P. A., and Ellar, D. J. (1996) *J. Mol. Biol. 257*, 129−152.
15. Gazit, E., and Shai, Y. (1993) *Biochemistry 32*, 12363−12371.
16. Ward, E. S., Ellar, D. J., and Chilcott, C. N. (1988) *J. Mol. Biol. 202*, 527−535.
17. Szabó, E., Murvai, J., Fábián, P., Fábián, F., Hollósi, M., Kajtár, J., Buzás, Z., Sajgó, M., S., P., and Asbóth, B. (1993) *Int. J. Pept. Protein Res. 42*, 527−532.
18. Gazit, E., Oren, Z., and Shai, Y. (1995) *Phytoparasitica 23*, 78.
19. Shai, Y., Bach, D., and Yanovsky, A. (1990) *J. Biol. Chem. 265*, 20202−20209.
20. Shai, Y. (1995) *Trends Biochem. Sci. 20*, 460−464.
21. Gazit, E., Lee, W. J., Brey, P. T., and Shai, Y. (1994) *Biochemistry 33*, 10681−10692.
22. Crickmore, N., Bone, E. J., and Ellar, D. J. (1990) *Aspects Appl. Biol. 24*, 17−24.
23. Al-yahyaee, S. A. S., and Ellar, D. J. (1995) *Microbiology 141*, 3141−3148.
24. Rapaport, D., and Shai, Y. (1991) *J. Biol. Chem. 266*, 23769−23775.
25. Mayer, L. D., Hope, M. J., and Cullis, P. R. (1986) *Biochim. Biophys. Acta 858*, 161−168.
26. Schwarz, G., Gerke, H., Rizzo, V., and Stankowski, S. (1987) *Biophys. J. 52*, 685−692.
27. Rizzo, V., Stankowski, S., and Schwarz, G. (1987) *Biochemistry 26*, 2751−2759.
28. Beschiaschvili, G., and Seelig, J. (1990) *Biochemistry 29*, 52−58.
29. Loew, L. M., Rosenberg, I., Bridge, M., and Gitler, C. (1983) *Biochemistry 22*, 837−844.
30. Strahilevitz, J., Mor, A., Nicolas, P., and Shai, Y. (1994) *Biochemistry 33*, 10951−10960.
31. Rapaport, D., and Shai, Y. (1992) *J. Biol. Chem. 267*, 6502−6509.
32. Stankowski, S., and Schwarz, G. (1990) *Biochim. Biophys. Acta 1025*, 164−172.
33. Pouny, Y., Rapaport, D., Mor, A., Nicolas, P., and Shai, Y. (1992) *Biochemistry 31*, 12416−12423.
34. Li, J. D., Carroll, J., and Ellar, D. J. (1991) *Nature 353*, 815−821.
35. Gazit, E., Boman, A., Boman, H. G., and Shai, Y. (1995) *Biochemistry 34*, 11479−11488.
36. White, S. H. (1994) *Membrane Proteins Structure, Experimental Approach*, Oxford University Press, Oxford.
37. Li, M., Jan, Y. N., and Jan, L. Y. (1992) *Science 257*, 1225−1230.
38. Lemmon, M. A., and Engelman, D. M. (1994) *Q. Rev. Biophys. 27*, 157−218.
39. Popot, J. L., and Engelman, D. M. (1990) *Biochemistry 29*, 4031−4037.

BI9707584